UHPLC-Orbitrap mass spectrometric characterization of organic aerosol from a central European city (Mainz, Germany) and a Chinese megacity (Beijing)

Kai Wang[a,b], Yun Zhang[a], Ru-Jin Huang[b,*], Junji Cao[b], Thorsten Hoffmann[a,**]

[a] Institute of Inorganic and Analytical Chemistry, Johannes Gutenberg University of Mainz, Duesbergweg 10–14, 55128, Mainz, Germany
[b] Key Lab of Aerosol Chemistry and Physics, Institute of Earth Environment, Chinese Academy of Sciences, Xi'an, 710061, China

GRAPHICAL ABSTRACT
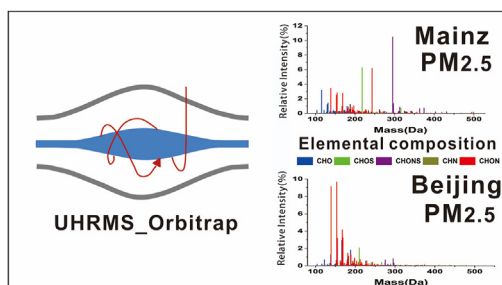
ARTICLE INFO

ABSTRACT

Fine urban aerosol particles with aerodynamic equivalent dimeter $\leq 2.5\,\mu m$ ($PM_{2.5}$) were collected in Mainz (a city within the Rhine-Main area, the third largest metropolitan region in Germany) and Beijing (Chinese megacity). A solvent mixture of acetonitrile-water was used to extract the organic aerosol fraction (OA) from the particle samples. The extracts were analyzed by an ultrahigh resolution mass spectrometer (UHRMS) Orbitrap coupled with ultra-high-performance liquid chromatography (UHPLC) both in the negative and positive ion mode. The number of compounds observed in Beijing is a factor of 2–10 higher compared to Mainz. The clear differences on chemical composition of OA in the two cities were observed. The majority of organics in Beijing OA is characterized by lower elemental H/C and O/C ratio but a higher degree of unsaturation and a larger aromaticity equivalent (X_C) compared to Mainz OA, suggesting that aromatics, which are related to direct combustion compounds (e.g., oxidized polycyclic aromatic hydrocarbon (PAH)), play an important role for OA in Beijing. A significant number of organosulfates (OSs) with long-carbon chain and low degree of unsaturation were observed in Beijing OA, indicating that long-chain alkanes emitted by vehicle might be their precursors.

1. Introduction

Organic aerosol (OA) constitutes a substantial fraction (20–90%) of submicrometer aerosol mass (Jimenez et al., 2009; Kroll et al., 2011) and influences air quality, climate, and human health (Hallquist et al., 2009; Poschl, 2005). Previous studies have shown that OA contains a variety of organic species, including hydrocarbons, alcohols, aldehydes, carboxylic acids, organosulfates and organonitrates. However, only

about 10–30% of OA has been chemically specified so far (Hoffmann et al., 2011). A better understanding of the chemical composition, properties and reactivity of OA are therefore important for assessing the effects of atmospheric aerosols. Since the thousands of compounds in OA covers a very large chemical space with respect to molecular mass, functional group distribution and polarity at trace level concentrations (Lin et al., 2012a; Noziere et al., 2015), characterization of OA is a challenging analytical task.

With the development of mass spectrometric techniques, considerable advances have been made over the past decade in terms of a better understanding of OA. The Aerodyne aerosol mass spectrometer (AMS) has been widely used to measure OA elemental composition and to study the sources and atmospheric processes (e.g., oxidation state) of OA (Canagaratna et al., 2015; Dall'Osto et al., 2015; Lee et al., 2015). However, the use of 70 eV electron ionization of the AMS leads to a high degree of fragmentation of OA and therefore difficulties in the identification and quantification of individual organics. Several approaches have been developed recently to introduce soft ionization techniques for OA studies, including atmospheric pressure chemical ionization (APCI) and electrospray ionization (ESI) (Hoffmann et al., 2011; Noziere et al., 2015). Especially ultrahigh resolution mass spectrometry (UHRMS) coupled with ESI allows the characterization of complex organic mixtures at the molecular level (Lin et al., 2012a; Nizkorodov et al., 2011; Rincón et al., 2012; Wang and Schrader, 2015). Fourier transform ion cyclotron (FTICR), Orbitrap and high-resolution quadrupole time-of-flight (HR-Q-TOF) are the three major high-resolution mass analyzers (Noziere et al., 2015). Due to the high mass resolving power ($\geq 40,000$) and high mass accuracy (≤ 5 ppm), the UHRMS techniques can detect thousands of individual organic aerosol components and provide their accurate chemical composition for each analysis. A recent review by Nizkorodov et al. (2011) shows that UHRMS analysis of secondary OA from smog chamber studies and aerosol samples collected from e.g., biomass burning, forest, rural and urban environment can provide improved understanding of the molecular composition and fundamental chemical transformations of OA. However, UHRMS analysis is instrumentally demanding and UHRMS studies of urban OA are still very scarce. Previous studies focused on the characterization of bulk OA or a group of specific compounds. For example, Lin et al. (2012a) characterized the element composition of humic-like substances in the Pearl River Delta Region, China. Tao et al. (2014) reported the analysis of organosulfates (OSs) in OA from Shanghai and Los Angeles. Wang et al. (2016) studied the OSs in three Chinese cities. Wang et al. investigated the month and diurnal variation of the OA chemical composition in Shanghai. Rincon et al.(Rincón et al., 2012) characterized the chemical composition of OA collected in different seasons at Cambridge, UK. Reemtsma et al.(T. et al., 2006) and Roach et al. (2010) studied the OA from Riverside, CA and Mexico city, respectively.

Over the past decade, particulate air pollution has become a serious environmental problem in China. Severe and persistent haze pollution occurred frequently in China in recent winters, particularly in megacities and urban complexes (Huang et al., 2014). Very recent studies show that outdoor air pollution, mostly by $PM_{2.5}$, leads to 3.3 million premature deaths per year worldwide, predominantly in Asia (Lelieveld et al., 2015). The yearly mass concentrations of $PM_{2.5}$ often exceed the WHO guideline concentration of $10\,\mu g\,m^{-3}$, even in many European urban areas. Given that about 55–75% of population lives in urban areas in China and European countries (European Environment Agency), a better understanding of the chemical composition, sources and atmospheric processes of aerosol in urban areas is important. This is particularly true for the OA fraction as it is much more complex and uncertain than the inorganic aerosol fraction. In this study, $PM_{2.5}$ samples were collected from Beijing (the capital of China with more than 20 million residents) and Mainz (a city within the Rhine-Main area, the third largest metropolitan region in Germany with more than 5.8 million population). However, the two urban regions experience very different natural and anthropogenic influences and it is worthwhile to investigate the similarities and differences in the OA composition in these two citie. Therefore, the organic fraction of the $PM_{2.5}$ samples in Beijing and Mainz were analyzed using UHPLC-Orbitrap MS in both negative and positive polarity and the difference in OA chemical composition is discussed.

2. Methodology

2.1. Sample collection and preparation

24-h integrated urban $PM_{2.5}$ samples were collected in Beijing (6 samples) and Mainz (3 samples). For the six Beijing samples, three were collected from 7 to 12 January 2014, during a relatively clean period with $PM_{2.5}$ mass concentrations between 32 and 38 $\mu g\,m^{-3}$ (sample ID: BJL (Beijing Low)). The other three samples were collected from 15 to 23 January 2014, during a severe haze pollution period with high $PM_{2.5}$ mass concentrations of 197–319 $\mu g\,m^{-3}$ (sample ID: BJH (Beijing High)). The three Mainz samples were taken from 15 to 28 January 2015 with relatively low $PM_{2.5}$ concentrations of 20–28 $\mu g\,m^{-3}$ (sample ID: MZL (Mainz Low)). The Beijing samples were collected on prebaked quartz-fiber filters (8 × 10 inch) using a high-volume sampler at a flow rate of 1.05 $m^3\,min^{-1}$, while the Mainz samples were collected on borosilicate glass fiber coated with fluorocarbon filters (Ø 70 mm, Pallflex T60A20, Pall Life Science, USA) using a low-volume sampler at a flow rate of 38.3 $L\,min^{-1}$. At each sampling site field blank samples were taken. The filter samples were stored at $-20\,°C$ until analysis. It should be noted that the $PM_{2.5}$ samples in Mainz and Beijing were collected in two consecutive years. An influence of year-to-year variability due to changing meteorological conditions cannot be excluded, however, both periods were wintertime periods with a similar regional scenario (Chang et al., 2017).

Portions of the filters (1.08–19.23 cm^2, corresponding to around 600 μg particle mass in each extracted filter) were extracted with 1.5 mL acetonitrile-water (8/2, v/v) in an ultrasonic bath for 30 min. The extraction step was repeated twice with 1 mL of the extraction solution. Then the combined extracts were filtered with a 0.2 μm Teflon syringe filter to remove insoluble particulate matter. Afterwards the solvent mixture was evaporated to dryness under a gentle stream of nitrogen. The residual was dissolved in 500 μL acetonitrile-water (1/9, v/v) for subsequent analysis.

2.2. UHRMS analysis

The analysis of the filter extracts was carried out using an ultrahigh resolution mass spectrometer (Q-Exactive mass spectrometer; Thermo Scientific, Germany) coupled to an UHPLC system (Dionex UltiMate 3000, Thermo Scientific, Germany). A Hypersil Gold column (C18, 50 × 2.0 mm, 1.9 μm particle size, Thermo Scientific, Germany) was used for separation. Eluent A (ultrapure water with 2% acetonitrile and 0.04% formic acid) and eluent B (acetonitrile with 2% ultrapure water) were used in a gradient mode with a flow rate of 500 $\mu L\,min^{-1}$. The optimized gradient was as follows: 0–1.5 min 2% B, 1.5–2.5 min from 2% to 20% B, 2.5–5.5 min 20% B, 5.5–6.5 min from 20% to 30% B, 6.5–7.5 min from 30% to 50% B, 7.5–8.5 min from 50% to 98% B, 8.5–11.0 min 98% B, 11.0–11.05 min from 98% to 2% B, 11.05–11.1 min 2% B. Each sample extract was measured in triplicate with an injection volume of 20 μL.

The Q Exactive mass spectrometer was equipped with a heated ESI source at 120 °C in the negative ion mode (ESI-) and 150 °C in the positive ion mode (ESI +). It was operated with 40 psi sheath gas, 20 psi auxillary gas, 320 °C capillary temperature and -3.3 kV spray voltage in the ESI- mode and 4.0 kV spray voltage in the ESI + mode. The mass spectrometer was calibrated with standard solution for ESI- and ESI+, respectively (See supporting information, SI). Mass spectra of all samples were acquired in both ESI- and ESI + in the mass range between $m/$

Table 1
The number of overall peaks observed in UHRMS, the number of assigned reasonable formulas and the relative abundance of each subgroup depending on their UHPLC chromatographic peaks (%), number-weighted average values of molecular weight, elemental ratios and DBE, and the isomer fraction in each subgroup.

Polarity and subgroup	Number of overall peak[a]	Number of formulas[b]	%	MW (Da)	H/C	O/C	DBE	Isomer fraction (%)
MZL								
total (−)	1961 (70%)	1081 (100%)	100	243	1.23	0.62	5.38	61
CHO-		347 (32%)	23	206	1.05	0.44	6.13	70
CHON-		376 (35%)	40	239	1.06	0.56	6.52	57
CHOS-		166 (15%)	15	241	1.66	0.78	2.51	51
CHONS-		192 (18%)	22	318	1.54	0.91	4.26	61
total (+)	5053 (57%)	1955 (100%)	100	225	1.34	0.27	5.76	61
CHO +		446 (23%)	13	215	1.07	0.33	7.02	64
CHN +		302 (15%)	11	177	1.33	0.00	5.93	79
CHON +		1103 (56%)	74	236	1.42	0.28	5.34	60
CHONS +		104 (6%)	2	292	1.65	0.68	4.29	11
BJL								
total (−)	3950 (78%)	2597 (100%)	100	241	1.22	0.51	5.85	72
CHO-		937 (36%)	24	217	0.98	0.34	7.29	81
CHON-		799 (31%)	53	230	0.96	0.50	7.28	68
CHOS-		494 (19%)	16	256	1.81	0.63	2.02	70
CHONS-		367 (14%)	7	305	1.57	0.81	4.26	57
total (+)	13,168 (72%)	7473 (100%)	100	229	1.26	0.19	6.73	80
CHO +		1705 (23%)	22	238	1.11	0.24	7.33	80
CHN +		1298 (17%)	35	199	1.12	0.00	8.01	92
CHON +		3848 (52%)	40	225	1.24	0.19	6.71	82
CHONS +		622 (8%)	3	292	2.10	0.42	2.52	41
BJH								
total (−)	6745 (72%)	3941 (100%)	100	244	1.19	0.45	6.07	78
CHO-		1718 (44%)	35	223	0.93	0.34	7.76	89
CHON-		842 (21%)	48	221	0.92	0.50	7.24	73
CHOS-		831 (21%)	12	280	1.74	0.51	2.26	80
CHONS-		550 (14%)	5	292	1.56	0.59	4.74	48
total (+)	28,696 (75%)	17,596 (100%)	100	235	1.28	0.21	6.75	89
CHO +		3990 (23%)	21	226	1.08	0.22	7.27	91
CHN +		2831 (16%)	39	210	1.14	0.00	8.16	96
CHON +		8400 (48%)	36	229	1.20	0.21	7.15	90
CHONS +		2375 (13%)	4	302	2.04	0.44	2.74	71

[a] Values in the parentheses are the percentage of peaks that can be assigned with unambiguous fomulas.
[b] Values in the parentheses are the percentage of different subgroups among the assigned reasonable formulas.

z 80 and m/z 500 with a resolving power of 70,000 @ m/z 200. The field blank filters were analyzed to correct for the background spectra. The mass accuracy of the measurements was < 3 ppm.

2.3. UHRMS data processing

Data were analyzed by a non-target screening approach using a commercially available software (SIEVE®, Thermo Scientific, Germany). This software provides the core functionality of MS data processing: peak detection, background subtraction and molecular formula assignment. The processing steps and settings are described in the following. A threshold intensity value of 1×10^5 arbitrary units in the two-dimensional space of the retention time window from 0 to 11.05 min and m/z from 80 to 500 was applied to all measurements. The software automatically searched the ions with their peak abundance above the threshold intensity value and only ions with peak abundance in the ambient samples 3 times greater than those in the blank samples were retained. After that, the molecular formulas of observed individual peaks were assigned by SIEVE with following constraints: #12C: 1 to 39, #1H: 1 to 72, #16O: 0 to 20, #14N: 0 to 7, #32S: 0 to 4 and #35Cl: 0 to 2 with mass tolerance of ± 2 ppm. In ESI + mode, 0–1 of Na was also included in the formula calculation because of the high tendency of sodium to form adducts with polar organic molecules. In addition, the isotope signals and ion-adducts (e.g., M-H + ACN) were checked and removed. Furthermore, to eliminate the chemically unreasonable formulas, the identified formulas

were constrained by setting H/C, O/C, N/C, S/C and Cl/C ratios in the ranges of 0.3–3, 0–3, 0–1.3, 0–0.8 and 0–0.8, respectively (Kind and Fiehn, 2007; Lin et al., 2012a; Wozniak et al., 2008). The resulting neutral formulas with a non-integer or negative double bond equivalent (DBE) or elemental composition which disobey the nitrogen rule for even electron ions were also removed. It should be noted that only molecular formulas observed in all three samples for each sample ID were considered for further calculation and discussion. The peak abundance of a compound in each sample ID corresponded to the average area of its chromatographic peak in the three filter samples and was blank-corrected. The DBE value was calculated by Eq. (1) for elemental composition $C_cH_hO_oN_nS_sCl_x$:

$$DBE = c - \frac{(h + x)}{2} + \frac{n}{2} + 1 \tag{1}$$

Additionally, the aromaticity equivalent (X_C) was used to improve the identification and characterization of aromatic and condensed aromatic compounds in OA, which was described in detail by Yassine et al. (2014). The X_C value can be calculated by Eq. (2):

$$X_C = \frac{3(DBE - (DBE - (mN_O + nN_S))) - 2}{DBE - (DBE - (mN_O + nN_S))} \tag{2}$$

where 'm' and 'n' correspond to a fraction of oxygen and sulfur atoms in π-bond structure of a compound, which varied depending on the compound. If $DBE \leq mN_O + nN_S$ or $X_C \leq 0$, then X_C was defined as zero. Due to the extreme complexity of urban OA, we used m = n = 1

for the conservative calculation of the X_C, which means every oxygen and sulfur atom was considered as π-bond structure (e.g. ketone and thioketone).

The assigned elemental formulas were classified into six species, including CHO, CHN, CHON, CHOS, CHONS and "other". CHONS referred to compounds containing carbon, hydrogen, oxygen, nitrogen and sulfur. The other species were defined analogously, while "other" includes CHS, CHNS and chlorine-containing compounds, which represented very low intensity and are not discussed here.

Since the response of each organic species to the mass spectrometer varies greatly, the average molecular weight (MW), H/C, O/C and DBE values were number-weighted calculated by following equations (3)–(6) (Lin et al., 2012a):

$$MW = \sum MW_i / \sum N_i \qquad (3)$$

$$H/C = \sum H/C_i / \sum N_i \qquad (4)$$

$$O/C = \sum O/C_i / \sum N_i \qquad (5)$$

$$DBE = \sum DBE_i / \sum N_i \qquad (6)$$

where N_i is the number of individual molecular formula i.

3. Result and discussion

3.1. General characteristics

As shown in Table 1, 1961–28696 mass peaks were detected in this study and the majority (57%–78%) of these detected peaks could be assigned with unambiguous formulas with mass tolerance less than 2 ppm, reflecting the high mass resolution power and high mass accuracy of the UHRMS technique. 1081–1955 molecular formulas of organic compounds with various numbers of isomers for each formula were detected in Mainz samples, while around 2–10 times more molecular formulas (2597–17596) were observed in Beijing samples, indicating the high complex of Beijing OA. The number of molecular formulas in this study is much higher compared to other UHRMS studies used direct infusion (Kourtchev et al., 2016; Lin et al., 2012a, 2012b; Rincón et al., 2012) and a previous UHPLC-Orbitrap MS study (Wang et al., 2017). This can be explained because UHPLC not only separates a large number of isomers, it also reduces ion suppression by coelution. In addition, the use of the mixture of ACN/H$_2$O is more efficient for OA extraction, especially for the less polar compounds (e.g., aromatics), compared to pure water or methanol used in previous studies. Moreover, the high organic carbon concentration (around 200 μg/cm^2 in BJH) can significantly result in more organic compounds observed in BJH in this study. It should be noted that the number of detected organic compounds is highly depending on the threshold intensity values applied for background subtraction, which always vary in different studies.61–92% of molecular formulas in this study contains isomers, indicating that UHPLC technique is very important tool for the characterization of complex ambient OA. And a representative UHPLC chromatogram for the UHPLC performance is shown in Fig. S1 in the Supporting Information (SI).

Mass spectra of observed organic compounds were reconstructed in both ESI- and ESI+ (see Fig. 1). It should be noted that different organic species have different signal response in the mass spectrometer, so uncertainties exist when comparing the peak areas of organics in different subgroups. In this work, all species are assumed to have the same signal response when we compare peak areas of organics among different samples. A significant difference between ESI- and ESI+ is observed in terms of both the number and abundance of the detected compounds (Table 1 and Fig. 1). Except CHOS compounds, all other subgroups have much more formulas in ESI+ mode compared to ESI-mode, indicating the less ionization suppression for these compounds in
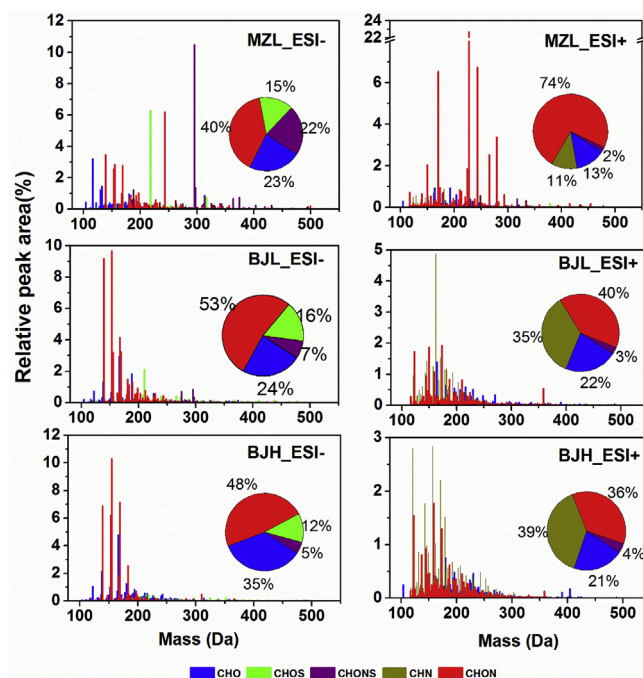
Fig. 1. Mass spectra of detected organic compounds in ESI- and ESI+. The pie chats are proportional to the peak areas of an organic compound subgroup in each sample.

ESI+. However, according to the peak abundance showed in Fig. 1, the abundance fractions of CHO, CHOS and CHONS compounds in ESI-mode are higher than that in ESI+ mode, while CHN compounds have higher abundance fraction in ESI+ and the fractions for CHON compounds vary depending on different samples. This is due to the different mechanisms between negative and positive ionization mode in the electrospray, where ESI- is especially sensitive to deprotonatable compounds (e.g., organic acids) and ESI+ is prone to protonatable compounds (e.g., organic basic compounds). In both Mainz and Beijing samples, CHON compounds show the highest total peak abundance of the detected compounds, which is consistent with other urban OA studies (Lin et al., 2012a; Rincón et al., 2012; Wang et al., 2017), indicating the importance of CHON compounds to the urban atmosphere.

Table 1 shows that the number-weighted averaged molecular weight of the total detected compounds is similar between Mainz and Beijing samples (241–244 Da in ESI- and 225–229 in ESI+). However, the number-weighted averaged H/C and O/C ratios of total compounds in Beijing samples are significantly lower compared to Mainz samples and the number-weighted averaged DBE in Beijing samples is higher than that in Mainz samples. This observation suggests that organics in Beijing OA are more condensed and unsaturated compared to Mainz OA and aromatics (e.g., oxidized PAH) have an important impact on the Beijing atmosphere.

3.2. CHO compounds

In this study, CHO compounds account for 23–35% of the peak abundance among the organic compounds detected in ESI-, while the fraction decreases to 13–22% in ESI+ mode (see Table 1), indicating CHO compound in this study are more sensitive in ESI- mode. This is consistent with a previous study from Lin et al. (2012a), which shows that most CHO compounds in OA contain carboxylic groups and are prone to deprotonate in ESI- mode. To further characterize the CHO compounds, van Krevelen (VK) and carbon oxidation state (OS$_c$) diagrams are produced. The VK diagram is often utilized to describe the compositional characteristics of complex organic mixtures. It provides a broad overview on their average composition and can be used to
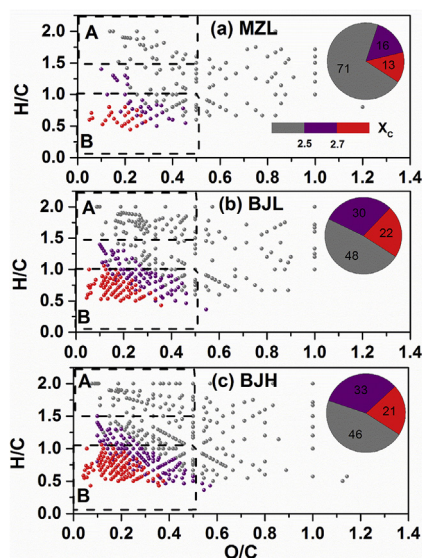
Fig. 2. The van Krevelen diagram for CHO compounds detected in ESI- mode. Areas 'A' and 'B' refer to aliphatic compounds and low-oxygen-containing aromatic hydrocarbons in organic aerosol, respectively. The colour bar denotes the aromaticity equivalent (gray with $X_C < 2.50$, purple with $2.50 \leq X_C < 2.70$ and red with $X_C \geq 2.70$). The pie chat shows the percentage of the number of each colour-coded compound in each sample. (For interpretation of the references to colour in this figure legend, the reader is referred to the Web version of this article.)

qualitatively classify different composition domains (Hockaday et al., 2009; Lin et al., 2012a; Rincón et al., 2012). The VK diagram for CHO compounds observed in ESI- is shown in Fig. 2, while the VK diagram for CHO compounds observed in ESI + is showed in Fig. S2. According to the H/C and O/C ratios, organic compounds can be divided into two different classes: aliphatic compounds with high H/C ratio (≥ 1.5) and low O/C ratios (≤ 0.5) (area A in Fig. 2) and low-oxygen-containing aromatic hydrocarbons with low H/C ratio (≤ 1.0) and low O/C ratio (≤ 0.5) (area B in Fig. 2) (Kourtchev et al., 2014). As can be seen in Fig. 2 (and Fig. S2), the majority of CHO compounds are located in the region A and B, which agrees well with previous urban OA studies (Kourtchev et al., 2014; Rincón et al., 2012). However, much more CHO compounds detected in Beijing samples were plotted in the region B, indicating that Beijing OA contains more low-oxygen-containing aromatic hydrocarbons. The number weighted averaged H/C and O/C ratios of CHO compounds detected in ESI- are 1.05 and 0.44, respectively, in Mainz samples, while lower H/C and O/C ratios (0.98 and 0.34 in BJL; 0.93 and 0.34 in BJH) are observed in Beijing samples. This result is also consistent with previous studies, for example, the H/C and O/C ratios are lower in the samples from the Pearl River Delta region in Southern China compared to those from Cambridge in the UK (Lin et al., 2012a; Rincón et al., 2012). The low H/C and O/C ratios indicate the unsaturated characteristics of CHO in urban aerosol samples from China. This is further confirmed by the aromaticity equivalent (X_C), which is a parameter determining the presence of aromatics ($X_C \geq 2.5$) and condensed aromatics ($X_C \geq 2.7$) (Yassine et al., 2014). As shown in the pie chart of Fig. 2, the fractions of aromatics and condensed aromatics are about 2 times and 1.7 times higher, respectively, in Beijing than in Mainz. The large difference in chemical characteristics of CHO compounds in Beijing and Mainz is likely associated with the different emission sources and/or atmospheric processes.

The carbon oxidation state (OS_C), introduced by Kroll et al. (2011) is another parameter used to describe the composition of a complex mixture of organics experiencing dynamic oxidation processes. OS_C can be calculated for each molecular formula of CHO compounds identified in the mass spectra following Eq. (7).
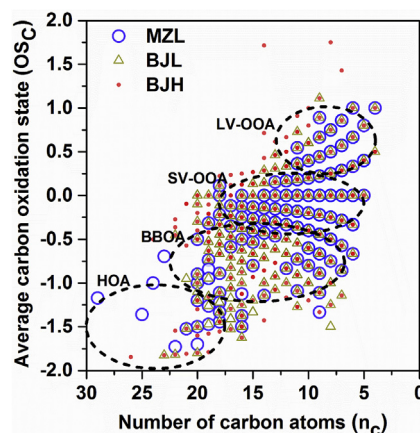
Fig. 3. Carbon oxidation state plots for CHO compounds detected in ESI- mode. The black dash ovals area marked as HOA, BBOA, SV-OOA and LV-OOA correspond to hydrocarbon-like organic aerosol, biomass burning organic aerosol, semivolatile and low-volatility organic aerosol.

$$OS_C \approx 2\,O/C - H/C \qquad (7)$$

Fig. 3 shows the overlaid OS_C as a function of carbon number for samples from Beijing and Mainz. Consistent with previous studies (Kourtchev et al., 2015, 2016; Wang et al., 2017), the majority of molecules in the CHO subgroup have OS_C between -1.5 and $+ 1$ with number of carbon atoms up to 30. The molecules with OS_C between -1 and -2 with 18 or more carbon atoms are suggested to be associated with hydrocarbon-like organic aerosol (HOA). The molecules with OS_C between -1.25 and -0.25 with 7–23 carbon atoms are associated with biomass burning organic aerosol (BBOA) directly emitted into the atmosphere. The molecules with OS_C between -0.5 and $+ 0.25$ with 5–18 carbon atoms are associated with semi-volatile oxygenated organic aerosol (SV-OOA), while the molecules with OS_C between $+0.25$ and $+ 1.0$ with 4–13 carbon atoms are associated with low-volatility oxygenated organic aerosol (LV-OOA) as defined by Kroll et al. (2011). As shown in Fig. 3, a large majority of CHO molecules are attributed to SV-OOA for both Beijing and Mainz samples, indicating the importance of atmospheric oxidation and aging in OA production. Significantly more BBOA associated molecules are obtained in Beijing compared to Mainz, reflecting the enhanced biomass burning activities in Beijing and surrounding areas (Cheng et al., 2013; Elser et al., 2016; Huang et al., 2014; Zhang et al., 2008). It should be noted that coal combustion is also an important OA source (Elser et al., 2016; Huang et al., 2014; Zhang et al., 2013, 2016), which is not discussed here due to the lack of source characterization with UHRMS study.

3.3. CHON compounds

A large amount of organic nitrogen compounds has been observed in fog water, continental precipitation as well as aerosol samples (Altieri et al., 2009; Jiang et al., 2016; Lin et al., 2012a; Mazzoleni et al., 2010). In this study, 376–842 of CHON- compounds (CHON compounds detected in ESI-) and 1103–8400 of CHON + compounds (CHON compounds detected in ESI +) were determined. The peak area of CHON- accounts for 40% in Mainz samples and it increases to 74% for CHON +. On the contrary, the peak area fractions of CHON- in Beijing samples (53% in BJL and 48% in BJH) are higher compared to that for CHON + (40% in BJL and 36% in BJH). This observation indicates that most CHON compounds in Mainz samples contain amino functional groups, which are prone to be protonated in ESI + mode, while CHON compounds in Beijing samples contain more nitro groups, which are preferentially to be deprotonated in ESI- mode.

The CHON compounds are further classified into different subgroups based on the O/N ratios. Fig. 4 shows the relative contribution
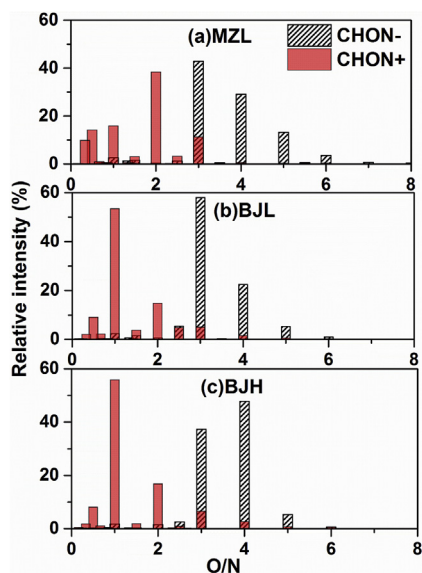
Fig. 4. Classification of CHON compounds into different subgroups according to O/N ratios in their molecules. The y-axis indicates the relative contribution of each subgroup to the sum of CHON compounds peak intentities observed in the ESI- and ESI + modes, respectively.

of each subgroup to the sum of CHON peak intensities observed in ESI + and ESI- mode. Compounds in the subgroups with O/N < 3 are preferentially detected in ESI + mode, again likely due to the presence of reduced nitrogen containing functional groups (e.g., amines). Interestingly, in ESI + mode, a large fraction (~40%) of CHON + compounds have O/N ratio of 2 for samples from Mainz, while compounds with O/N ratio of 1 dominate (~55%) for samples from Beijing regardless of the pollution level. This is an indication that CHON + compounds in Beijing OA contain more reduced nitrogen atoms, which could be produced from a minor pyrolytic and oxidative processing (e.g., smoldering burning) of N-heterocycle compounds (e.g., imidazole) (Lin et al., 2012a). The number-weighted averaged DBE for CHON + compounds is 5.34 in Mainz samples, while higher averaged DBEs (6.71 in BJL and 7.15 in BJH) are observed in Beijing samples, indicating CHON + compounds in Beijing OA are more unsaturated. This is further confirmed by the VK diagram in Fig. S3, which shows that much more CHON + compounds in Beijing samples are suggested to be low-oxygen-containing aromatic hydrocarbons in area B. And, the pie chat in Fig. S3 shows that the fractions of aromatics and condensed aromatics in Beijing samples are about 1.25 times and 6 times higher, respectively, compared to Mainz samples. It indicates that reduced nitrogen-containing aromatic precursors have more influence on CHON + compounds in Beijing than in Mainz. Another interesting subgroup of CHON compounds are those compounds with O/N ≥ 3, which are preferentially observed in ESI- mode, likely associated with the nitrooxy (-ONO$_2$) or oxygenated nitrooxy group (O/N ≥ 4). The majority of CHON- compounds has O/N ratio of 3 or 4, indicating that besides the nitrooxy group most CHON- compounds contain additionally not more than one oxidized group. This observation is confirmed by the modified VK diagram for CHON- compounds in Fig. S4 (in which the VK diagram was constructed by plotting the H/C ratio versus the (O-3N)/C ratio instead of O/C ratio), showing a large number of CHON- compounds are observed with low (O-3N)/C ratio between 0 and 0.2. However, compared to the CHON- compounds in MZL and BJL samples dominating with O/N ratio of 3, the CHON- compounds in BJH samples are dominated with O/N ratio of 4, suggesting CHON- compounds undergo relatively higher oxidized process in polluted air. Consistent with the CHON + compounds, the number-weighted averaged DBE (see Table 1) and the fraction of aromatics of CHON- compounds (see Fig. S4) in Beijing samples are higher than those in Mainz

samples, indicating that nitrogen containing aromatics are more important precursors in Beijing OA, which agrees well with Wang et al.'s study (Wang et al., 2017) showing many nitrooxy-aromatic compounds (e.g., nitrophenol) with high abundance observed in the OA of Shanghai. It should be noted that only a small fraction of CHON compounds is observed in both ESI + and ESI- modes (see overlapped bar in Fig. 4). Actually this fraction of CHNO compounds could consist of amino acids, which contain both acidic (-COOH) and basic (-NH$_2$) functional groups and which have been identified in biomass burning and fossil fuel combustion emissions (Barbaro et al., 2011; Mace, 2003).

3.4. CHN compounds

The CHN compounds can be detected only in ESI, which are very likely associated with nitrile and amine species (Lin et al., 2012a). The number-weighted averaged molecular weight of CHN compounds is the smallest in all subgroups. However, the number-weighted averaged DBE (5.93–8.16) of CHN compounds is the highest, indicating that this group of molecules is highly unsaturated. CHN compounds accounts for around 11% of the total peak abundance in Mainz sample, while it is more than three times higher in Beijing samples (35% in BJL and 39% in BJL), suggesting that CHN compounds have more important impact on Beijing OA compared to Mainz OA.

Fig. 5 shows the Kendrick mass defect (KMD) diagram for the CHN compounds observed in Mainz and Beijing samples. The KMD diagram is commonly used to investigate the relationship among a large set of molecular formulas in the UHRMS study (Hughey et al., 2001; Kendrick, 1963; Lin et al., 2012a; Rincón et al., 2012). Here, we set the molar mass of CH$_2$ to exactly 14 u as the reference mass for calculating the Kendrick mass (KM) following Eq. (8) and the KMD is defined as the difference between the nominal mass and the KM as shown in Eq. (9).

$$KM(CH_2) = mass \times [mass\ CH_2]/mass\ CH_2 \tag{8}$$

$$KMD(CH_2) = [mass] - KM(CH_2) \tag{9}$$

where brackets refer to the nominal mass obtained by rounding the mass to the nearest integer. When the KMD of a compound is plotted *vs.* its neutral molecular weight, homologous series of compounds differing only by CH$_2$ fall on horizontal lines and are clearly distinguishable. As can be seen in Fig. 5, the majority of CHN compounds belong to
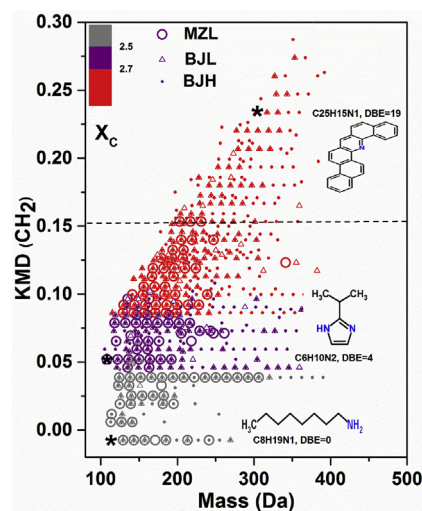
Fig. 5. Kendrick mass defect diagram of CHN compounds detected in ESI + mode. The colour bar denotes the aromaticity equivalent (gray with X$_C$ < 2.50, purple with 2.50 ≤ X$_C$ < 2.70 and red with X$_C$ ≥ 2.70). The element composition, DBE and a potential chemical structure for the first compound (the black asterisk) of three homologous series are illustrated in the figure. (For interpretation of the references to colour in this figure legend, the reader is referred to the Web version of this article.)

members of several different homologous series. However, compared to the homologous series of CHN compounds in Mainz samples, the homologous series in Beijing samples often have a higher number of members with larger molecular weights. This could be explained by more primary biological aerosol particles with long chain aromatic amines or N-heterocycle compounds in Beijing atmosphere (Jiang et al., 2014; Rincón et al., 2012). The X_C values suggest that most CHN compounds are condensed aromatics ($X_C \geq 2.7$) and aromatics ($X_C \geq 2.5$). To facilitate the imagination of possible chemical species within Fig. 5, the elemental composition, the DBE and a potential chemical structure for the first compound of three homologous series are also illustrated in the figure, representing a condensed aromatic species, an aromatic compound and a non-aromatic species. In previous MS/MS studies of CHN compounds (Laskin et al., 2009; Lin et al., 2012a; Simoneit et al., 2003), these nitrogen containing aromatic compounds are suggested to be alkaloids with one or two nitrogen atoms embedded into five-membered (e.g., pyrazole, imidazole, and their derivatives) or six-membered rings (e.g., pyridazine and their derivatives), which are likely formed during biomass burning from dialkanoic acids and ammonia. It is worth noting that a significant number of CHN compounds with 12–23 DBE and 15–29 carbon atoms (those above the dash line in Fig. 5) are exclusively present in Beijing samples. These compounds are assigned to polycyclic aromatic N-heterocycle hydrocarbons (PANH) with four or more aromatic rings, which are strong mutagens and potential human carcinogens. This result is consistent with a previous study in which several PANH with 4–8 aromatic rings were observed in ambient organic aerosol from Beijing (Jiang et al., 2014).

3.5. Sulfur compounds (CHOS and CHONS subgroups)

A large number of S-containing organic compounds have been observed in urban and rural OA (Jiang et al., 2016; Tao et al., 2014; Wang et al., 2016, 2017). In this study, 166–831 CHOS formulas were determined in ESI- mode. 86–93% of CHOS formulas are assigned to possess a molecular composition with O/S ratio ≥ 4, suggesting they represent organosulfates (OSs), which is consistent with previous studies (Tao et al., 2014; Wang et al., 2016). The number-weighted average molecular weight of CHOS compounds in Beijing samples (250 Da in BJL and 280 Da in BJH) is larger than that (241 Da) in Mainz samples. In contrast, the number-weighted average DBE in Beijing samples (2.02 in BJL and 2.26 in BJH) is lower than that (2.51) in Mainz samples. Moreover, the DBE vs. carbon number diagram in Fig. S5 shows that more CHOS compounds with low DBE and high carbon numbers were observed in Beijing samples, indicating that CHOS compounds with longer carbon chain and lower degree of unsaturation make an important contribution to Beijing OSs. This result is similar to a previous study (Tao et al., 2014), which revealed that the OSs in Shanghai have longer aliphatic carbon chains and lower degree of unsaturation than the OSs in Los Angeles. As observed in smog chamber studies (Riva et al., 2016), the OSs with high molecular weight and low degree of unsaturation can be formed from long-chain alkanes (e.g., dodecane) emitted from combustion sources. Besides the CHOS compounds, the other S-containing organics are assigned to be CHONS compounds, which are also prone to be measured in ESI- mode. The CHONS compounds account for around 22% of the total peak abundance in ESI- mode in the Mainz samples, while the fraction decreases to 5–7% in the samples from Beijing. The compound with the formula $C_{10}H_{17}O_7NS$, which has been identified as an α-pinene-derived nitrooxy-OSs, shows the highest concentration in Mainz (see Fig. 1), while its concentration is much smaller in Beijing, indicating the important role of monoterpene precursor on CHONS compounds in Mainz OA. In Mainz and BJL samples, 61–65% of detected CHONS- formulas have the O/(4S + 3N) ratio ≥ 1, allowing their assignment to nitrooxy-OSs with both –OSO$_3$H and –ONO$_2$ groups. However, in BJH samples, only 29% of the CHONS- formulas are suggested to be nitrooxy-Oss. To further

understand the chemical properties of these CHONS compounds, MS/MS analysis should be performed in the future.

4. Conclusion and implication

In this study, we applied the UHPLC-Orbitrap MS for the analysis of the organic fraction of PM$_{2.5}$ samples from one European city Mainz and one Chinese city Beijing. Roughly 18000 organic compounds were identified based on unambiguous elemental composition in the urban OA, while the number of organics in Beijing samples are around 2–10 times more than Mainz samples. The information of these organic compounds can enrich the database of the molecular composition of OA in urban regions. 61–92% of the detected organics have more than one isomer, indicating that the UHPLC separation is important for the OA characterization and suggested to be applied prior to the mass spectrometer for the identification or quantification of individual organic substances in the OA in future studies.

The chemical characteristics of OA in Mainz and Beijing shows clear differences. The organic species of CHO, CHON and CHN in Beijing OA have lower elemental H/C and O/C (except CHN) but higher DBE and Xc compared to Mainz OA, demonstrating that organics in Beijing OA are highly unsaturated. The Van Krevelen and KMD diagrams show that much more mono/poly aromatics were observed in Beijing OA, suggesting that they are combustion related compounds. The majority of CHOS compounds are suggested to be OSs, while OSs in the two cities have different molecular characteristics showing that many OS with low DBE and high carbon numbers were only detected in Beijing OA. Most CHONS compounds were observed in low concentrations in PM$_{2,5}$ (MZL and BJL). These elemental compositions can be assigned to represent mostly nitrooxy-OS. Only 29% of CHONS compounds collected during high PM$_{2.5}$ episodes (BJH) are suggested to be nitrooxy-OSs, point out the large differences in the chemical composition of CHONS compounds in the heavily and in the less polluted atmosphere. In future studies more detailed MS studies (e.g. MS/MS analysis) should be performed for a better understanding of the molecular structures, sources or formation pathways of these compounds. As shown in this study, biogenic and anthropogenic precursors have a different influence on the Beijing OA and Mainz OA. Therefore, dedicated smog chamber experiments with mixtures of biogenic (e.g., α-pinene) and anthropogenic (e.g., naphthalene) precursors might be conducted to better understand their influence on OA formation in urban regions.

Appendix A. Supplementary data

Supplementary data related to this article can be found at http://dx.doi.org/10.1016/j.atmosenv.2018.06.036.

References

Altieri, K.E., Turpin, B.J., Seitzinger, S.P., 2009. Composition of dissolved orgnic nitrogen in continental precipitation investigated by ultra-high resolution FT-ICR mass spectrometry. Environ. Sci. Technol. 43, 6.
Barbaro, E., Zangrando, R., Moret, I., Barbante, C., Cescon, P., Gambaro, A., 2011. Free

amino acids in atmospheric particulate matter of Venice. Italy. Atmo. Environ 45, 5050–5057.

Canagaratna, M.R., Jimenez, J.L., Kroll, J.H., Chen, Q., Kessler, S.H., Massoli, P., Hildebrandt Ruiz, L., Fortner, E., Williams, L.R., Wilson, K.R., Surratt, J.D., Donahue, N.M., Jayne, J.T., Worsnop, D.R., 2015. Elemental ratio measurements of organic compounds using aerosol mass spectrometry: characterization, improved calibration, and implications. Atmos. Chem. Phys. 15, 253–272.

Chang, Y., Deng, C., Cao, F., Cao, C., Zou, Z., Liu, S., Lee, X., Li, J., Zhang, G., Zhang, Y., 2017. Assessment of carbonaceous aerosols in Shanghai, China – Part 1: long-term evolution, seasonal variations, and meteorological effects. Atmos. Chem. Phys. 17, 9945–9964.

Cheng, Y., Engling, G., He, K.B., Duan, F.K., Ma, Y.L., Du, Z.Y., Liu, J.M., Zheng, M., Weber, R.J., 2013. Biomass burning contribution to Beijing aerosol. Atmos. Chem. Phys. 13, 7765–7781.

Dall'Osto, M., Paglione, M., Decesari, S., Facchini, M.C., O'Dowd, C., Plass-Duellmer, C., Harrison, R.M., 2015. On the origin of AMS "cooking organic aerosol" at a rural site. Environ. Sci. Technol. 49, 13964–13972.

Elser, M., Huang, R.-J., Wolf, R., Slowik, J.G., Wang, Q., Canonaco, F., Li, G., Bozzetti, C., Daellenbach, K.R., Huang, Y., Zhang, R., Li, Z., Cao, J., Baltensperger, U., El-Haddad, I., Prévôt, A.S.H., 2016. New insights into PM$_{2.5}$ chemical composition and sources in two major cities in China during extreme haze events using aerosol mass spectrometry. Atmos. Chem. Phys. 16, 3207–3225.

European Environment Agency, http://www.eea.europa.eu/themes/urban.

Hallquist, M., Wenger, J.C., Baltensperger, U., Rudich, Y., Simpson, D., Claeys, M., Dommen, J., Donahue, N.M., George, C., Goldstein, A.H., Hamilton, J.F., Herrmann, H., Hoffmann, T., Iinuma, Y., Jang, M., Jenkin, M.E., Jimenez, J.L., Kiendler-Scharr, A., Maenhaut, W., McFiggans, G., Mentel, T.F., Monod, A., Prevot, A.S.H., Seinfeld, J.H., Surratt, J.D., Szmigielski, R., Wildt, J., 2009. The formation, properties and impact of secondary organic aerosol: current and emerging issues. Atmos. Chem. Phys. 9, 5155–5236.

Hockaday, W.C., Purcell, J.M., Marshall, A.G., Baldock, J.A., Hatcher, P.G., 2009. Electrospray and photoionization mass spectrometry for the characterization of organic matter in natural waters: a qualitative assessment. Limnol Oceanogr. Meth. 7, 81–95.

Hoffmann, T., Huang, R.J., Kalberer, M., 2011. Atmospheric analytical chemistry. Anal. Chem. 83, 4649–4664.

Huang, R.J., Zhang, Y., Bozzetti, C., Ho, K.F., Cao, J.J., Han, Y., Daellenbach, K.R., Slowik, J.G., Platt, S.M., Canonaco, F., Zotter, P., Wolf, R., Pieber, S.M., Bruns, E.A., Crippa, M., Ciarelli, G., Piazzalunga, A., Schwikowski, M., Abbaszade, G., Schnelle-Kreis, J., Zimmermann, R., An, Z., Szidat, S., Baltensperger, U., El Haddad, I., Prevot, A.S., 2014. High secondary aerosol contribution to particulate pollution during haze events in China. Nature 514, 218–222.

Hughey, C.A., Hendrickson, C.L., Rodgers, R.P., Marshall, A.G., 2001. Kendrick mass defect spectrum: a compact visual analysis for ultrahigh-resolution broadband mass spectra. Anal. Chem. 73, 4676–4681.

Jiang, B., Liang, Y., Xu, C., Zhang, J., Hu, M., Shi, Q., 2014. Polycyclic aromatic hydrocarbons (PAHs) in ambient aerosols from Beijing: characterization of low volatile PAHs by positive-ion atmospheric pressure photoionization (APPI) coupled with Fourier transform ion cyclotron resonance. Environ. Sci. Technol. 48, 4716–4723.

Jiang, B., Kuang, B.Y., Liang, Y., Zhang, J., Huang, X.H.H., Xu, C., Yu, J.Z., Shi, Q., 2016. Molecular composition of urban organic aerosols on clear and hazy days in Beijing: a comparative study using FT-ICR MS. Environ. Chem. 13, 888.

Jimenez, J.L., Canagaratna, M.R., Donahue, N.M., Prevot, A.S.H., Zhang, Q., Kroll, J.H., DeCarlo, P.F., Allan, J.D., Coe, H., Ng, N.L., Aiken, A.C., Docherty, K.S., Ulbrich, I.M., Grieshop, A.P., Robinson, A.L., Duplissy, J., Smith, J.D., Wilson, K.R., Lanz, V.A., Hueglin, C., Sun, Y.L., Tian, J., Laaksonen, A., Raatikainen, T., Rautiainen, J., Vaattovaara, P., Ehn, M., Kulmala, M., Tomlinson, J.M., Collins, D.R., Cubison, M.J., Dunlea, E.J., Huffman, J.A., Onasch, T.B., Alfarra, M.R., Williams, P.I., Bower, K., Kondo, Y., Schneider, J., Drewnick, F., Borrmann, S., Weimer, S., Demerjian, K., Salcedo, D., Cottrell, L., Griffin, R., Takami, A., Miyoshi, T., Hatakeyama, S., Shimono, A., Sun, J.Y., Zhang, Y.M., Dzepina, K., Kimmel, J.R., Sueper, D., Jayne, J.T., Herndon, S.C., Trimborn, A.M., Williams, L.R., Wood, E.C., Middlebrook, A.M., Kolb, C.E., Baltensperger, U., Worsnop, D.R., 2009. Evolution of organic aerosols in the atmosphere. Science 326, 1525–1529.

Kendrick, E., 1963. A mass scale based on CH2 = 14.0000 for high resolution mass spectrometry of organic compounds. Anal. Chem. 35, 2146–2154.

Kind, T., Fiehn, O., 2007. Seven Golden Rules for heuristic filtering of molecular formulas obtained by accurate mass spectrometry. BMC Bioinf. 8.

Kourtchev, I., O'Connor, I.P., Giorio, C., Fuller, S.J., Kristensen, K., Maenhaut, W., Wenger, J.C., Sodeau, J.R., Glasius, M., Kalberer, M., 2014. Effects of anthropogenic emissions on the molecular composition of urban organic aerosols: an ultrahigh resolution mass spectrometry study. Atmos. Environ. 89, 525–532.

Kourtchev, I., Doussin, J.F., Giorio, C., Mahon, B., Wilson, E.M., Maurin, N., Pangui, E., Venables, D.S., Wenger, J.C., Kalberer, M., 2015. Molecular composition of fresh and aged secondary organic aerosol from a mixture of biogenic volatile compounds: a high-resolution mass spectrometry study. Atmos. Chem. Phys. 15, 5683–5695.

Kourtchev, I., Godoi, R.H.M., Connors, S., Levine, J.G., Archibald, A.T., Godoi, A.F.L., Paralovo, S.L., Barbosa, C.G.G., Souza, R.A.F., Manzi, A.O., Seco, R., Sjostedt, S., Park, J.-H., Guenther, A., Kim, S., Smith, J., Martin, S.T., Kalberer, M., 2016. Molecular composition of organic aerosols in central Amazonia: an ultra-high-resolution mass spectrometry study. Atmos. Chem. Phys. 16, 11899–11913.

Kroll, J.H., Donahue, N.M., Jimenez, J.L., Kessler, S.H., Canagaratna, M.R., Wilson, K.R., Altieri, K.E., Mazzoleni, L.R., Wozniak, A.S., Bluhm, H., Mysak, E.R., Smith, J.D., Kolb, C.E., Worsnop, D.R., 2011. Carbon oxidation state as a metric for describing the chemistry of atmospheric organic aerosol. Nat. Chem. 3, 133–139.

Laskin, A., Smith, J.S., Laskin, J., 2009. Molecular characterization of nitrogen-containing organic compounds in biomass burning aerosols using high-resolution mass spectrometry. Environ. Sci. Technol. 43, 3764–3771.

Lee, T., Choi, J., Lee, G., Ahn, J., Park, J.S., Atwood, S.A., Schurman, M., Choi, Y., Chung, Y., Collett, J.L., 2015. Characterization of aerosol composition, concentrations, and sources at Baengnyeong Island, Korea using an aerosol mass spectrometer. Atmos. Environ. 120, 297–306.

Lelieveld, J., Evans, J.S., Fnais, M., Giannadaki, D., Pozzer, A., 2015. The contribution of outdoor air pollution sources to premature mortality on a global scale. Nature 525, 367–371.

Lin, P., Rincon, A.G., Kalberer, M., Yu, J.Z., 2012a. Elemental composition of HULIS in the Pearl River Delta Region, China: results inferred from positive and negative electrospray high resolution mass spectrometric data. Environ. Sci. Technol. 46, 7454–7462.

Lin, P., Yu, J.Z., Engling, G., Kalberer, M., 2012b. Organosulfates in humic-like substance fraction isolated from aerosols at seven locations in East Asia: a study by ultra-high-resolution mass spectrometry. Environ. Sci. Technol. 46, 13118–13127.

Mace, K.A., 2003. Water-soluble organic nitrogen in Amazon Basin aerosols during the dry (biomass burning) and wet seasons. J. Geophys. Res. 108.

Mazzoleni, L.R., Ehrmann, B.M., Sheng, X.H., Marshall, A.G., Collett, J.L., 2010. Water-soluble atmospheric organic matter in fog exact masses and chemical formula identification by ultrahigh-resolution fourier transform ion cyclotron resonance mass spectrometry. Environ. Sci. Technol. 44, 8.

Nizkorodov, S.A., Laskin, J., Laskin, A., 2011. Molecular chemistry of organic aerosols through the application of high resolution mass spectrometry. Phys. Chem. Chem. Phys. 13, 3612–3629.

Noziere, B., Kalberer, M., Claeys, M., Allan, J., D'Anna, B., Decesari, S., Finessi, E., Glasius, M., Grgic, I., Hamilton, J.F., Hoffmann, T., Iinuma, Y., Jaoui, M., Kahnt, A., Kampf, C.J., Kourtchev, I., Maenhaut, W., Marsden, N., Saarikoski, S., Schnelle-Kreis, J., Surratt, J.D., Szidat, S., Szmigielski, R., Wisthaler, A., 2015. The molecular identification of organic compounds in the atmosphere: state of the art and challenges. Chem. Rev. 115, 3919–3983.

Poschl, U., 2005. Atmospheric aerosols: composition, transformation, climate and health effects. Angew. Chem. Int. Ed. 44, 7520–7540.

Rincón, A.G., Calvo, A.I., Dietzel, M., Kalberer, M., 2012. Seasonal differences of urban organic aerosol composition - an ultra-high resolution mass spectrometry study. Environ. Chem. 9, 298.

Riva, M., Da Silva Barbosa, T., Lin, Y.-H., Stone, E.A., Gold, A., Surratt, J.D., 2016. Chemical characterization of organosulfates in secondary organic aerosol derived from the photooxidation of alkanes. Atmos. Chem. Phys. 16, 11001–11018.

Roach, P.J., Laskin, J., Laskin, A., 2010. Molecular characterization of organic aerosols using nanospray-desorption/electrospray ionization-mass spectrometry. Anal. Chem. 82, 7979–7986.

Simoneit, B.R.T., Rushdi, A.I., Bin Abas, M.R., Didyk, B.M., 2003. Alkyl amides and nitriles as novel traces for biomass burning. Environ. Sci. Technol. 37, 16–21.

T, R, THESe, A., Venkatachari, P., Xia, X.Y., Hopke, P.K., Springer, A., Linscheid, M., 2006. Identification of fulvic acids and sulfated and nitrated analogues in atmospheric aerosol by electrospray ionization fourier transform ion cyclotron resonance mass spectrometry. Anal. Chem. 78, 8299–8304.

Tao, S., Lu, X., Levac, N., Bateman, A.P., Nguyen, T.B., Bones, D.L., Nizkorodov, S.A., Laskin, J., Laskin, A., Yang, X., 2014. Molecular characterization of organosulfates in organic aerosols from Shanghai and Los angeles urban areas by nanospray-desorption electrospray ionization high-resolution mass spectrometry. Environ. Sci. Technol. 48, 10993–11001.

Wang, X., Schrader, W., 2015. Selective analysis of sulfur-containing species in a heavy crude oil by deuterium labeling reactions and ultrahigh resolution mass spectrometry. Int. J. Mol. Sci. 16, 30133–30143.

Wang, X.K., Rossignol, S., Ma, Y., Yao, L., Wang, M.Y., Chen, J.M., George, C., Wang, L., 2016. Molecular characterization of atmospheric particulate organosulfates in three megacities at the middle and lower reaches of the Yangtze River. Atmos. Chem. Phys. 16, 2285–2298.

Wang, X.K., Hayeck, N., Brüggemann, M., Yao, L., Chen, H.F., Zhang, C., Emmelin, C., Chen, J.M., George, C., Wang, L., 2017. Chemical characterization of organic aerosol in: a study by ultrahigh-performance liquid chromatography coupled with Orbitrap mass spectrometry. J. Geophys. Res. 11703–11722.

Wozniak, A.S., Bauer, J.E., Sleighter, R.L., Dickhut, R.M., Hatcher, P.G., 2008. Technical Note: molecular characterization of aerosol-derived water soluble organic carbon using ultrahigh resolution electrospray ionization Fourier transform ion cyclotron resonance mass spectrometry. Atmos. Chem. Phys. 8, 5099–5111.

Yassine, M.M., Harir, M., Dabek-Zlotorzynska, E., Schmitt-Kopplin, P., 2014. Structural characterization of organic aerosol using Fourier transform ion cyclotron resonance mass spectrometry: aromaticity equivalent approach. Rapid Commun. Mass Spectrom. 28, 2445–2454.

Zhang, T., Claeys, M., Cachier, H., Dong, S., Wang, W., Maenhaut, W., Liu, X., 2008. Identification and estimation of the biomass burning contribution to Beijing aerosol using levoglucosan as a molecular marker. Atmos. Environ. 42, 7013–7021.

Zhang, R., Jing, J., Tao, J., Hsu, S.C., Wang, G., Cao, J., Lee, C.S.L., Zhu, L., Chen, Z., Zhao, Y., Shen, Z., 2013. Chemical characterization and source apportionment of PM$_{2.5}$ in Beijing: seasonal perspective. Atmos. Chem. Phys. 13, 7053–7074.

Zhang, J.K., Cheng, M.T., Ji, D.S., Liu, Z.R., Hu, B., Sun, Y., Wang, Y.S., 2016. Characterization of submicron particles during biomass burning and coal combustion periods in Beijing, China. Sci. Total Environ. 562, 812–821.